[CANCER RESEARCH 62, 3466–3476, June 15, 2002]

Parallel Analysis of Sporadic Primary Ovarian Carcinomas by Spectral Karyotyping, Comparative Genomic Hybridization, and Expression Microarrays[1, 2]

Jane Bayani, James D. Brenton,[3] Pascale F. Macgregor, Ben Beheshti, Monique Albert, Dhani Nallainathan, Jana Karaskova, Barry Rosen, Joan Murphy, Stephanie Laframboise, Brent Zanke,[4] and Jeremy A. Squire[5]

Ontario Cancer Institute [J. B., B. B., D. N., J. K., B. Z., J. A. S.] and Departments of Medical Oncology and Hematology [J. D. B., B. Z.] and Gynecological Oncology [B. R., J. M., S. L.], Princess Margaret Hospital, University Health Network; Departments of Medical Biophysics [B. Z., J. A. S.] and Laboratory Medicine and Pathobiology [J. B., B. B., J. A. S.], University of Toronto; and Microarray Centre [P. F. M., M. A.], Clinical Genomics Center, University Health Network, Toronto M5G 2M9, Canada

ABSTRACT

Analysis of ovarian carcinomas has shown that karyotypes are often highly abnormal and cannot be identified with certainty by conventional cytogenetic methods. In this study, 17 tumors derived from 13 patients were analyzed by a combination of spectral karyotyping (SKY), comparative genomic hybridization (CGH), and expression microarrays. Within the study group, a total of 396 chromosomal rearrangements could be identified by SKY and CGH analysis. When the distribution of aberrations was normalized with respect to relative genomic length, chromosomes 3, 8, 11, 17, and 21 had the highest frequencies. Parallel microarray expression studies of 1718 human cDNAs were used to analyze expression profiles and to determine whether correlating gene expression with chromosomal rearrangement would identify smaller subsets of differentially expressed genes. Within the entire set of samples, microarray expression analysis grouped together poorly differentiated tumors irrespective of histological subtype. For three patients, a comparison between genomic alterations and gene expression pattern was performed on samples of primary and metastatic tumors. Their common origin was demonstrated by the close relationship of both the SKY and CGH karyotypes and the observed profiles of gene expression. In agreement with the pattern of genomic imbalance observed for chromosome 3 in ovarian cancer, the relative expression profile with respect to a normal ovary exhibited a contiguous pattern of reduced expression of genes mapping to the 3p25.5–3p21.31 and increased expression of genes from 3q13.33–3q28. This study demonstrates that SKY, CGH, and microarray analysis can in combination identify significantly smaller subsets of differentially expressed genes for future studies.

INTRODUCTION

Ovarian cancer is the leading cause of death from a gynecological malignancy and the fourth leading cause of cancer death among North American women. Response to treatment is generally poor, and the 5-year survival rate for all cases, at best, is only 50%. This poor outcome is because most ovarian cancers are asymptomatic, not detected until the disease has metastasized beyond the ovary and has a high cytological grade. Although the mechanisms of the disease are still poorly understood, there is a causal association with mutations of *BRCA1* and *BRCA2* in familial disease (1). Sporadic ovarian cancer, which makes up >85% of all cases, rarely shows mutations in *BRCA1* and *BRCA2* (1). Acquired mutations of *p53* have been frequently identified among the serous subtype (2), whereas mutations of *PTEN* occur in the endometrioid subtypes (3), suggesting that they arise through distinct developmental pathways.

Cytogenetic analyses of ovarian carcinomas show both simple numerical and structural changes and complex aberrant changes (4–11). A cytogenetic survey of 244 ovarian carcinomas identified a clustering of chromosomal translocation breakpoints occurring in the regions 1p1*, 1q1*, 1p2*, 1q2*, 1p3*, 1q3, 3p1*, 1q4*, 6q1*, 6p2, 6q2, 7p1, 7p2*, 11p1*, 11q2*, 12p1, 12q2*, 13p1, and 19q1 [where the asterisk (*) denotes the most commonly involved regions of chromosomal rearrangement] (12–14). The presence of translocations in the regions shown above was associated with reduced patient survival. Chromosomal alterations in the regions 1p1 and 3p1 were found to confer an independent deleterious effect. One disadvantage of this study was that individual breakpoints were assigned to very large chromosomal regions (containing several hundred genes), making specific recurrent structural aberration identification difficult.

In recent years, molecular cytogenetic studies such as CGH[6] (15) and SKY (16) have demonstrated their power in identifying recurrent chromosomal aberrations. To date, CGH has been widely used (17–25) in studying ovarian carcinomas and has identified increased copy numbers at 1q32, 3q26, 8q24.1-q24.2, 20q13.2-qter and frequent chromosomal losses identified at 5q21, 9q, 17p, 17q12-q21, 4q26-q31, 16q, and 22q. Sites of amplification have been identified at 7q36, 8q24.1-q24.2, 3q26.3, 17q25, 19q13.1-q13.2, and 20q13.2-qter by CGH.

Microarray analysis is a relatively new technique (26, 27), which allows the simultaneous expression analysis of thousands of genes from a single sample. Profiling and clustering of data from solid tumors have suggested new molecular classifications in lymphoma and breast cancer and generated hypotheses for metastatic markers in melanoma. Similar approaches have identified deregulated genes in ovarian cancer (13, 28–32); however, the relationship between these candidates and prognosis or classification is not yet clear. Microarray studies on nonovarian malignancies show that cancers with identical histological phenotype have marked differences in global expression patterns. Given this variability, we hypothesized that correlating expression analysis with chromosomal dosage change or rearrangement would allow better identification of key genetic changes in ovarian cancer.

In this study, we have performed parallel analysis using SKY, CGH, and microarray methods on a small cohort of ovarian carcinomas. Our objective was to identify a correlation between deviations in gene expression and chromosomal abnormalities identified by SKY

Received 6/14/01; accepted 4/30/02.

The costs of publication of this article were defrayed in part by the payment of page charges. This article must therefore be hereby marked *advertisement* in accordance with 18 U.S.C. Section 1734 solely to indicate this fact.

[1] Supported in part by the Ovarian Fashion Show Committee.

[2] Supplementary data for this article are available at *Cancer Research Online* (http://cancerres.aacrjournals.org).

[3] Present address: Department of Oncology (Box 193), School of Clinical Medicine, University of Cambridge, Addenbrooke's Hospital, Cambridge CB2 2QQ, United Kingdom.

[4] Present address: The Cross Cancer Institute, 11560 University Avenue, Edmonton, Alberta, T6G 1Z2 Canada.

[5] To whom requests for reprints should be addressed, at Ontario Cancer Institute, Division of Cellular and Molecular Biology, 610 University Avenue, Room 9-721, Toronto, Ontario, M5G 2M9 Canada. Phone: (416) 946-4509; Fax: (416) 920-5413; E-mail: jeremy.squire@utoronto.ca.

[6] The abbreviations used are: CGH, comparative genomic hybridization; SKY, spectral karyotyping; EST, expressed sequence tag; OPN, osteopontin; DAPI, 4′,6-diamidino-2-phenylindole; RT-PCR, reverse transcription-PCR; IGFBP, insulin-like growth factor binding protein; VEGF, vascular endothelial growth factor.

and CGH, in combination with a pilot microarray expression profiling of ovarian carcinoma.

MATERIALS AND METHODS

Ovarian Tissue and Tumor Samples

Seventeen tumors from 13 patients were obtained at the time of surgery and promptly processed for DNA and RNA extraction and, where possible, short-term culture for cytogenetic preparation. The study group consisted of 9 serous tumors (including 1 serous carcinosarcoma), 6 endometrioid tumors, 1 clear cell tumor, and 1 mucinous tumor of low malignant potential as determined by standard histopathological classification. In 4 patients, two distinct tumor samples were obtained. OCA3A/OCA3B, OCA13A/OCA13B, OCA21A/OCA21B are paired primary/metastasis samples. OCA15A/B tumors were obtained from the right and left ovaries, respectively. The histopathological classification, age, stage, and grade of each tumor are summarized in Table 1. In all cases, except for OCA6 and OCA13A/B, the tumors obtained were from the first surgery and were untreated. Some patients received treatment at other institutions, and for others follow-up data are unavailable.

DNA and RNA Extraction

Seventeen tumor specimens were processed for DNA and RNA extraction. DNA extraction was performed using standard phenol:chloroform extract methods (33). Frozen tumor samples were rapidly minced on a −70°C stage, homogenized, and RNA was extracted using standard methods (34). Additional purification was performed using RNeasy columns (Qiagen, Mississauga, Ontario, Canada) following the manufacturer's protocol. RNA quality was evaluated by spectrophotometry and by electrophoresis on a 1% denaturing formaldehyde-agarose gel. RNA from 14 tumor samples derived from 9 ovarian patients (OCA2, OCA3A/B OCA5, OCA8, OCA9, OCA13A/B, OCA15A/B, OCA17, OCA19, and OCA21A/B) was found to be suitable for microarray expression analysis. DNA and RNA specimens were stored at −70°C until ready for use. RNA derived from nine cell lines, HL-60, K562, H226, COLO 205, OVCAR-3, Caki-1, PC-3, MCF7, and Hs 578T (American Type Tissue Culture Collection, Rockville, MA), were extracted, pooled in equal amounts, and used as the reference RNA for initial microarray expression analysis (35). Two reference normal ovarian RNA samples were used for a subset of microarray expression experiments. One RNA sample (Stratagene, La Jolla, CA) was derived from bulk-extracted normal margin to hemorrhagic

Table 1 *Summary of tumor specimens analyzed and CGH results*[a]

Patient information includes age, histology, grade, and stage of tumor. A full description of the SKY results as well as the CGH results can be accessed as supplementary information2 at the National Center for Biotechnology Information SKY and CGH Database (2001),7.

Case	Age	Histology	Grade	Stage	Status	CGH results
OCA1	55	Papillary serous adenocarcinoma	3/3	IV	First surgery Untreated	Normal
OCA2	56	Endometroid adenocarcinoma	2/3	III	First surgery Untreated	+1q32-qter,−3p,+3q,−4,+6q13–q23,−12p,−15,−17p11–p21,−18q11–q21, +20q,+X
OCA3A-primary	81	Papillary serous cystadenocarcinoma	3/3	III	First surgery Untreated	−2p26,+3q12-qter,−4q13-qter,+6p,+8q22-qter,−9q11–q31,+12p,+18,
OCA3B-metastasis						ND[a]
OCA5	66	Clear cell adenocarcinoma	NA[a]	I	First surgery Untreated	+5p14-pter,+8q,−11pter-q21,+12p12-pter,+X
OCA6	55	Papillary serous adenocarcinoma	ND	IIC	Second surgery 3 courses of treatment prior to surgery	Normal
OCA8	55	Papillary serous adenocarcinoma	2/3	II	First surgery Untreated	−1p22–p31,+1q,+2,−3p,+3q,−4,−5,+6p,−6q,+7q,+8q21-qter, −9,+15,+16p,+17q21-qter,+18q,+19,+20,−22
OCA9	64	Endometrioid adenocarcinoma	2/3	I	First surgery Untreated	Normal
OCA13A-primary	79	Endometrioid adenocarcinoma Poorly differentiated	3/3	III	Second surgery 3 courses of treatment prior to surgery	+1p34-pter,+1q,+2p15-q13,+3,−7p21-pter,+7q32–q35,+8q21–q22,+10q24–q25,+11q13,−11q22–q23,+12q11–q13,−17q21,−18q,+20p
OCA13B-metastasis						+1p34-pter,+1q,+2p15-q13,+3,+7q32–q35,−8p,+8q21–22,+10q24–q25, −11p12–p14,−11q22–q23-14q12–q14,−18q,+20p
OCA15A-right ovary	43	Endometrioid adenocarcinoma Poorly differentiated	3/3	III	First surgery Untreated	+1,−2q33–q37,−3p23-pter,+3q21-qter,−4q,+5p,+6p,+7q,+9q22-qter,+10p, −11p12–p15,+11q14–q23,+12q23–q24,−16q21-qter,−18,+19q
OCA15B-left ovary						+1,−3p24-pter,+3q21-qter,−4q,−6q22-qter,−7p21-pter,+7q,+10q11–q24, −12p12-pter,+12q23–24
OCA16	35	Mucinous Low malignant potential	3	NA	First surgery Untreated	Normal
OCA17	70	Papillary serous adenocarcinoma Moderately differentiated with some endometrioid components	2	III	First surgery Untreated	−1p35-pter,+2p24-pter,−3p26,+3q26-qter,−4q13–q25,+6q24,+7q21–q32,+8p22-q12,+8q24,10p13-pter,+12q,−14q11–q21,−15,+16q,+18q21–q22,+20p
OCA19	57	Carcinosarcoma serous Undifferentiated with mesenchymal components	NA	IB or II	First surgery Untreated	−1p21–p22,−3p24-pter,+3q,−4,−5p,+5q11–q13,−6q14-qter,+7q32-qter,+8q,−9,−13,−14,−15q13–q21,+16,+17p,+18p11–p13,+X
OCA21A-primary	50	Serous adenocarcinoma Poorly differentiated	NA	III	First surgery Untreated	−2q23-qter,−4,−6q21–q24,−7p21–p22.2,+7q34-qter,+8q23-qter,+9p,+20q, +Xq11–q13,+Xq25–q27
OCA21B-metastasis						−2q23-qter,−4,−6q21–q24,−7p21–p22.2,+7q34-qter,+8q23-qter,+9p,+20q, +Xq11–q13,+Xq25–q27

[a] ND, not done; NA, not available.

Table 2 *Integrated summary of CGH and SKY aberrations in ovarian cancer study group*

The number of SKY breakpoints (identified as circles in Fig. 2) and CGH imbalances (*bars* in Fig. 2) were enumerated to determine the overall level of aberration for each chromosome. Concordant SKY and CGH rearrangements were only counted once. To normalize the frequency of aberration per chromosome with respect to relative genomic size, an expected frequency of aberration was calculated using chromosome size data (37). The most frequently abnormal chromosomes are shown in bold.

Chromosome	CGH aberrations	SKY aberrations	Concordant SKY/CGH	Total number	Genome size (%)	Expected
1	8	27	1	34	8.060687	32.4
2	6	20	1	25	7.668303	30.8
3	**12**	**22**	**4**	**30**	**6.482927**	**26.0**
4	7	9	0	16	6.16345	24.8
5	6	13	1	18	5.774848	23.2
6	9	13	2	20	5.811804	23.3
7	9	12	1	20	5.139513	20.6
8	**8**	**36**	**4**	**40**	**4.528678**	**18.2**
9	5	7	0	12	4.176379	16.8
10	4	10	0	14	4.465997	17.9
11	**8**	**22**	**2**	**28**	**4.481724**	**18.0**
12	8	9	1	16	4.433076	17.8
13	1	8	0	9	3.83872	15.4
14	3	3	0	6	3.433542	13.8
15	4	14	1	17	3.144024	12.6
16	4	7	1	10	2.915522	11.7
17	**4**	**14**	**0**	**18**	**2.631862**	**10.6**
18	7	5	1	11	2.552577	10.3
19	2	7	0	9	2.489155	10.0
20	5	7	1	11	1.99552	8.0
21	**0**	**15**	**0**	**15**	**1.497536**	**6.0**
22	1	3	0	4	1.530352	6.1
X	4	9	0	13	4.871078	19.6
				394		

cyst from a 41-year-old donor, and the second sample (Ambion, Austin, TX) was also bulk extracted from a healthy 29-year-old donor who died of anoxia.

Preparation of Metaphase Spreads

Tumor specimens were finely minced and collagenase treated (Life Technologies, Inc., Gaithersburg, MD) for 24 h at 37°C in a CO_2 incubator. The following day, the disaggregated tissue was processed for short-term culture in α-MEM supplemented with FCS (20%; Sigma), penicillin/streptomycin (1%; Life Technologies, Inc.), and L-glutamine (1%; Life Technologies, Inc.). The cultures were harvested within 4 days using 0.1 μg/ml colcemid treatment (Life Technologies, Inc.) for 2–4 h, hypotonic treatment with 0.075 M KCl, and fixed in 3:1 methanol:acetic acid. The slides were prepared and aged for several days at room temperature.

SKY Method and Nomenclature

SKY analysis was carried out on metaphase slides aged for <1 month. The assay was carried out using the SKY Paint according to the manufacturer's instructions (ASI, Carlsbad, CA; Ref. 36). The full nomenclature describing the karyotypes is presented as supplementary information,[2] and is also summarized in the National Center for Biotechnology Information SKY and CGH Database (2001). These operations represent only the clonal aberrations.[7] A gain of a chromosome was described when identified in at least two metaphase spreads, a loss when identified in three or more cells, and a chromosomal rearrangement when identified in two or more cells. To assess the karyotype complexity, the number of cytogenetic abnormalities detected by SKY was determined by counting the aberrations described in the karyotype in each case according to the following criteria: Multiple copies of structural or numerical aberration were counted only once; in derivative chromosomes, each structural abnormality was counted once; and each breakpoint in complex rearrangements was counted once. In cases 13A/B, 15A/B, and 21A/B, where there are paired primary and metastatic samples, the stemline karyotype was counted once, with only the addition of the unique clonal changes in each of the primary and metastatic sample added to Fig. 2. Thus, the relative comparisons of overall structural aberrations and imbalances shown in Fig. 2 and summarized in Table 2 refer to the total number of SKY breakpoints and CGH copy number changes detected along the length of a given chromosome. In determining the mean number of breakpoints present between endometrioid and serous subtypes, the full karyotypes (*i.e.*, stemline and unique breakpoints) were averaged giving a total of 443 breakpoints for tumors OCA2, OCA3A, OCA8, OCA13A/B, OCA15A/B, and OCA21A/B.

CGH

Metaphase spreads from normal human lymphocytes were prepared using standard protocols (38). Ten to 12 images were captured using a Nikon Labophot-2 microscope equipped with an automatic filter wheel and an 83,000 filter set (Chroma, Brattleboro, VT) with single band pass exciter filters for UV/FITC (490 nm), DAPI (360 nm), and rhodamine (570 nm). Slides were analyzed using the Vysis Quips SmartCapture imaging system (Vysis, Downers Grove, Il) and analyzed using the Quips CGH/Karyotyper and Interpreter (Vysis). The lower and upper limit for a gain and loss was established by performing control CGH experiments with DNA derived from male and female normal tissue, and regions of imbalance were confirmed by reverse labeling where possible. On the basis of these findings, the cutoff values were set at 1.20 and 0.80, with a 95% confidence limit. Gene amplification was defined as gain ratios > 1.5. The regions of imbalance detected by CGH analysis are provided in Table 1 and are included as supplementary information together with details concerning rearrangements identified by SKY.[2]

Microarray Analysis

Microarrays used in this study were purchased from the Microarray Centre, University Health Network (Toronto, Ontario, Canada). These arrays contain 1718 human cDNAs selected from the Swissprot database, with 74 positive control and 74 negative control features. All features are spotted in duplicate for a total of 3840 spots. A complete list of the cDNA collection used for these arrays ("Human 1.7K2" and "Human 1.7K3") and protocols used for array construction can be found at the University Health Network Microarray Centre web site.[8] Human 1.7K2 and Human 1.7K3 contain the same set of human ESTs, and the difference is the cDNA spot locations for some ESTs. All reverse transcriptions (direct and indirect labeling) and hybridizations conditions are available.[9] Two series of microarray experiments were carried out as described below.

Microarray Analysis with a Nine Cell Line Reference RNA. For the microarray analysis of 13 tumor samples against RNA derived from a pool of nine cell lines, the RNA samples were labeled using amino-allyl indirect labeling, using a 2:1 ratio of amino-allyl dUTP:dTTP. Tumor RNAs were labeled with Cy5, and the pooled reference RNA was labeled with Cy3, followed by column purification (High Pure PCR Product Purification kit; Roche). The eluates were lyophilized and stored at −70°C. Duplicate arrays were hybridized for each tumor sample. For a subset of 4 tumor samples, there was sufficient RNA for comparisons to two normal ovarian reference RNAs. In these experiments, all RNAs were labeled using direct labeling. In one set of arrays, all 4 tumor RNAs and the Stratagene normal ovary RNA were labeled with Cy3, and the reference normal ovary RNA (Ambion) was labeled with Cy5.

Microarray Analysis Using a Normal Ovarian RNA Reference. In a second set of arrays, all tumor RNAs and the Stratagene normal ovary RNA were labeled with Cy3, and the reference RNA (Ambion) was labeled with Cy5 (dye switches) to account for possible labeling bias. Slides were scanned using either an Axon GenePix 4000A (Axon, Foster City, CA) or ScanArray 4000 scanner (Packard BioScience) dual laser scanner and quantified with GenePix Pro 3.0 software (Axon). Features that were not quantified because they were flagged bad or absent by GenePix Pro were manually reviewed for accuracy. Filtering, normalization of the raw data, and complete data analysis of the data sets were carried out with an algorithm developed in house that will be published elsewhere.[10] Briefly, each of the 16 subgrids on each array was independently normalized by equalizing the Cy3 intensities, with respect to the Cy5 intensities, while excluding features flagged bad or absent by GenePix

[7] Internet address: http://www.ncbi.nlm.nih.gov/sky/skyweb.cgi.

[8] Internet address: http://www.uhnres.utoronto.ca/services/microarray.

[9] Internet address: http://www.uhnres.utoronto.ca/services/microarray/protocols/index.html.

[10] B. Beheshti, I. Braude, P. Marrano, P. T. Thorner, M. Zielenska, and J. A. Squire, manuscript in preparation.

Pro. Other features excluded by the algorithm included saturated spots and spots with foreground:background intensity ratio < 2. The Cy5:Cy3 normalized intensity ratio was determined for each spot, and these values from the duplicate spots within each array were averaged. Subsequently, Cy5:Cy3 ratios for the same spots between replicate experiments of each sample were averaged together as a single project file. Finally, the project files representing each sample and its replicates were combined into a single text file for processing by the Cluster software package for hierarchical clustering, and the Treeview software was used for generating the graphical visualization of the clustering (39).[11] Clustering was performed on genes showing expression values present in ≥80% of samples. For the first series of microarray experiments, we used median centering of the genes and tumors to emphasize differences between tumors rather than changes with respect to the standard comparator RNA (39, 40). The agglomerative hierarchical clustering algorithm used in the Cluster software successively joins gene expression profiles to form a dendrogram based on their pairwise similarities. The same procedure is followed when clustering by experiment, *i.e.*, the similarity between each experiment is determined over the total number of genes as an average, and experiments with similar averages are grouped together (41). Two-dimensional hierarchical clustering first reorders genes and then reorders tumors based on similarities of gene expression between samples. The datasets used for hierarchical clustering generated by this study are available as tab-delimited format text files.[12] Custom software was also developed to automate retrieval of chromosome localizations of microarray cDNAs from the UniGene database (at present, build 144). This allowed for arrangement of cDNAs into sequential order in megabases along each chromosome. The mapping distribution of the 1718 human cDNAs (1.7K2 and 1.7K3) used in this study, as well as the software, to carry out retrieval of chromosomal localizations are available.[13]

Confirmation of Microarray Results by Semi-quantitative RT-PCR. cDNA was prepared from 20 ng of total RNA extracted from samples OCA17, OCA19, OCA21A, and OCA21B by reverse transcriptase-PCR using specific primers for the following genes using the Sigma One-Step RT-PCR kit (Sigma-Aldrich, St. Louis, MO): OPN (sense: 5′ACAGCATCGTCGGGACCAGA3′, antisense: 5′CATCCATCCACCTTCATCCACC3′); decorin (sense: 5′CAGTGTTCTGATTTGGGTCTGGAC3′, antisense: 5′CGTAAGGGAAGGAGGAAGACC3′); and ribosomal 60S (sense: CCGCCATAACAAGGACCGAAAGT3′, antisense: 5′ACCCGGCCGTCTTGTTTTCC3′). RT-PCR reactions were also run in parallel with PCR primer pairs for the 18S rRNA (Ambion) as an internal standard. The following reaction/cycling conditions were used: 45 min at 45°C; 3 min at 94°C; 30 cycles of 45 s at 94°C, 30 s at 55°C, and 1 min at 72°C; and 5 min at 72°C. An aliquot of each reaction was run onto a 1% agarose gel, and the gel was stained with ethidium bromide. The intensities of each band were quantified using a Gel Documentation AlphaImager System (Alpha Innotech, San Leandro, CA) and were normalized using the intensities obtained for the 18S internal standard. The results are displayed in Fig. A.[2, 14]

RESULTS

Overall SKY Analysis of Ovarian Carcinoma Study Group. Examples of SKY analysis are shown in Fig. 1, and a detailed summary of both SKY breakpoint distribution and CGH imbalance profiles is presented using international system for human cytogenetic nomenclature as supplementary material to this article and in Fig. 2. Of the 292 breakpoints shown in Fig. 2, 229 (78.4%) could be mapped to a precise band by a combination of SKY and DAPI banding analysis (42). Although no recurrent structural aberration was detected by SKY, the regions 1p11, 1q11, 2q23, 3p21, 3q11, 5p11, 5q11, 6p11-p12, 6q14, 8p11, 8q11–12, 8q22-q23, 11p11, 11q11, 11q23, 13p11, 13q11, and 21p11 were subject to more frequent rearrangement. There were four or more centromeric or pericentromeric rearrangements at chromosomes 6, 8, and 11. Of the 292 SKY breakpoints, the poorly differentiated tumors displayed an average of 52 breakages/tumor, and the well-differentiated tumors had an average of 27 breakages/tumor. Ploidy levels were near diploid or tetraploid in all of the tumors except the clear cell tumor (OCA5), which was found to be near triploid. Of the 17 tumors studied, only five (OCA1, OCA3B, OCA9, OCA16, and OCA17) either failed to provide adequate metaphase cells for SKY analysis or exhibited a normal karyotype. One tumor (OCA17) had chromosomal imbalances by CGH and a normal SKY karyotype, suggesting that the mitotically active metaphase population most likely represented normal cell contamination.

SKY Comparisons of Metastatic and Primary Ovarian Tumors. OCA15A/B were ovarian primary tumors presenting in both the right and left ovaries, respectively, and OCA3A/OCA3B, OCA13A/OCA13B, and OCA21A/OCA21B were paired primary/metastatic tumor samples. Of these, only OCA3B failed to produce adequate metaphases for pairwise comparisons. An example of the SKY generated karyotype and the corresponding CGH analysis of OCA13A is shown in Fig. 1*A*. For OCA15A/B, a majority of the ~40 clonal aberrations detected by SKY in the right and left ovary were concordant; however, the right ovary (OCA15A) possessed additional aberrations, including deletions at 1q22, 3p21, and 8p10 and complex rearrangements affecting chromosomes 2, 5, and 11 that were not detected in the left ovary (OCA15B). Similarly, the left ovary exhibited unique aberrations, including deletions at 2p11 and 11q11 and a translocation der(11)t(11;15)(p11;q12) not evident in the tumor present at the right ovary. OCA21A and OCA21B were primary and metastatic tumors, respectively. OCA21A was found to be tetraploid, whereas OCA21B was found to be diploid, but the majority of structural and numerical aberrations were concordant and duplicated in the primary tumor (Fig. 1, *B* and *C*). Examples of concordant deletions were present at Xp11, 6q15, and 10p11.2. Instances of concordant translocations were der(1)t(1;3)(p36;q24), der(8)t(8;11)(p21;p12), der(8)t(X;8)(q23;q22), der(10)del(10)(p11.2)t(10;11)(q21;q14q22), der(11)t(X;11)(p15;p21), der(21)t(11;21)(q11;p11), and a complex rearrangement involving breakpoints at 8q22::3p21→q24::17q22. However, several unique clonal rearrangements were detected in the metastatic tumor OCA21B such as the three translocations +der (1)t(1;18)(q41;q22), +der(8)t(7;8)(p12;p12?), der(13)t(9;13)(q21p12), and der (13)t(9;13)(p11;p11). Similarly for the tumor pair OCA13A and OCA13B, the majority of the ~68 aberrations found were common to both samples. Aberrations that were unique to the metastatic tumor OCA13B included del(X)(q11) and two translocations der(4)t(4;5)(q24;?p11), and der(18)t(18;20)(q11.2;?). In summary, it was possible to demonstrate by SKY that three of the four paired samples (OCA13A/B, OCA15A/B, and OCA21A/B) were closely related in terms of their pattern of cytogenetic aberration determined by SKY, and that this concordance indicates an origin from a common progenitor.

Chromosomal Aberrations Identified by both CGH and SKY. In Fig. 1*A*, a representative comparison between the CGH findings and SKY results using tumor OCA13A is shown. It can be seen that extensive areas of CGH gain on chromosomes 1, 2, 3, and X arise as a result of large unbalanced translocations detected by SKY. Smaller regions of CGH loss and gain are also detected in other chromosomal regions that appear to be generated by much smaller rearrangements. In cases where an unbalanced chromosomal rearrangement was determined by SKY, but the specific sub region could not be recognized because of a lack of identifiable banding information, CGH was used to infer the probable region of genomic imbalance. These data are illustrated for OCA13A in Fig. 1*A*, where a net gain was detected at 8q21-q22. SKY analysis detected aberrations on chromosome 8: der(8)t(8;10)(p11;p11); and chromosome 19: der(19)t(8;19)(?;p11),der

[11] Internet address: http://rana.lbl.gov.
[12] Internet address: http://www.utoronto.ca/cancyto/OVCA2001CR/.
[13] Internet address: http://www.utoronto.ca/cancyto/.
[14] Fig. A to be available as supplementary information on the web edition. RT-PCR analysis of OPN, decorin, and ribosomal 60S using ovarian cancer samples OCA17, OCA19, and OCA21A/B.

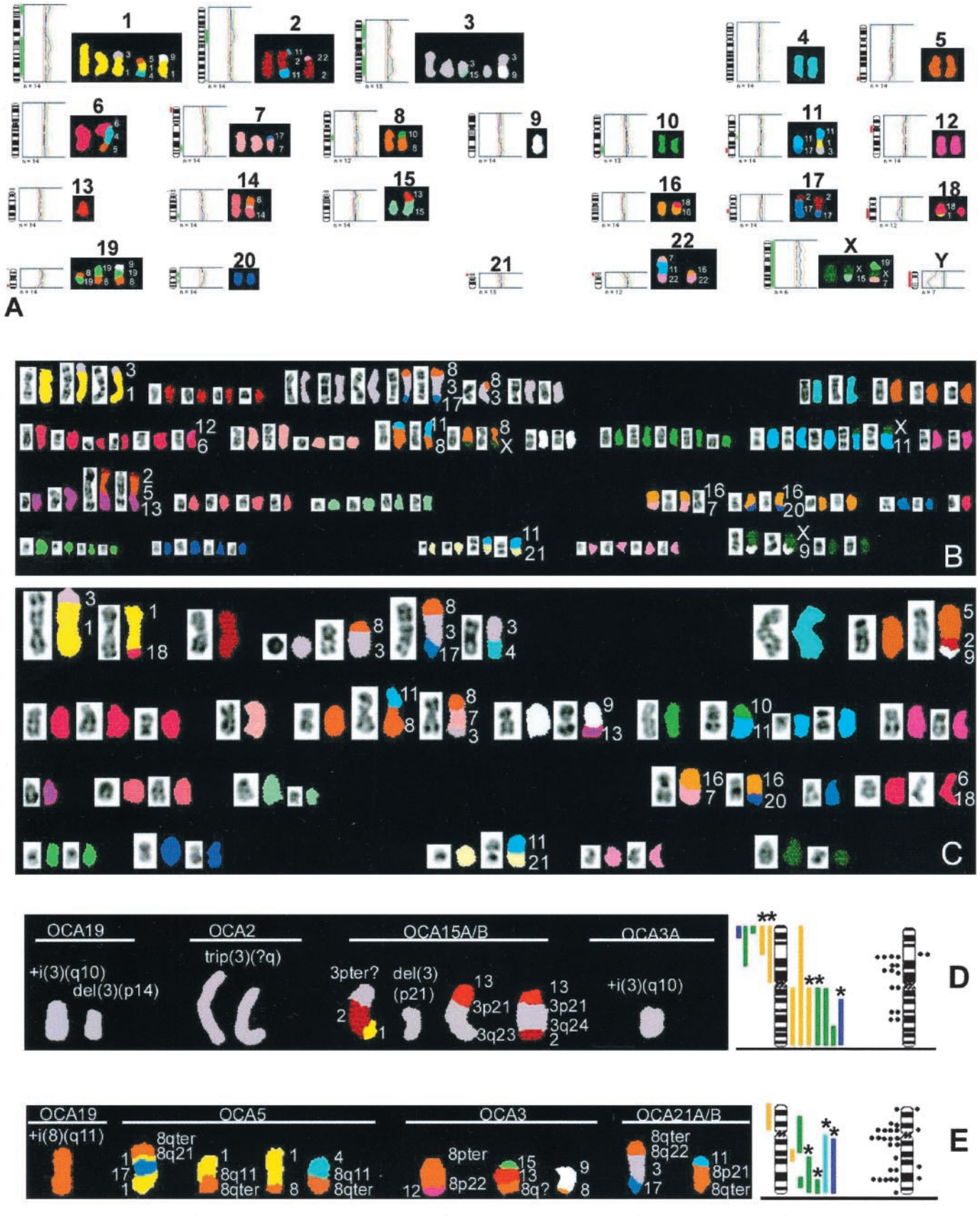

Fig. 1. SKY and CGH analysis of ovarian tumors. *A*, SKY and CGH analysis of OCA13A. Shown are the results of SKY and CGH analysis of a primary endometrioid tumor. The SKY karyogram illustrates the pseudocolored classified colors enabling better identification of regions of chromosomal transition. Illustrated beside the karyogram is the corresponding CGH profile identifying net chromosomal gains and losses as indicated by *green bars* and *red bars*, respectively. *B* and *C*, SKY analysis of OCA21A and OCA21B, respectively. Shown are the SKY karyograms of endometrioid tumors derived from the same patient, one the primary (OCA21A) and the second the metastasis (OCA21B). In these karyotypes, both the classified and inverted DAPI banding images are shown. The *panel* below illustrates the RGB (Red-Green-Blue) and inverted DAPI banding images of the metaphases karyotyped above. *D*, integrated CGH and SKY analysis for chromosome 3. Shown are the tumor specimens possessing net genomic changes on chromosome 3 (denoted by "*") that correlate

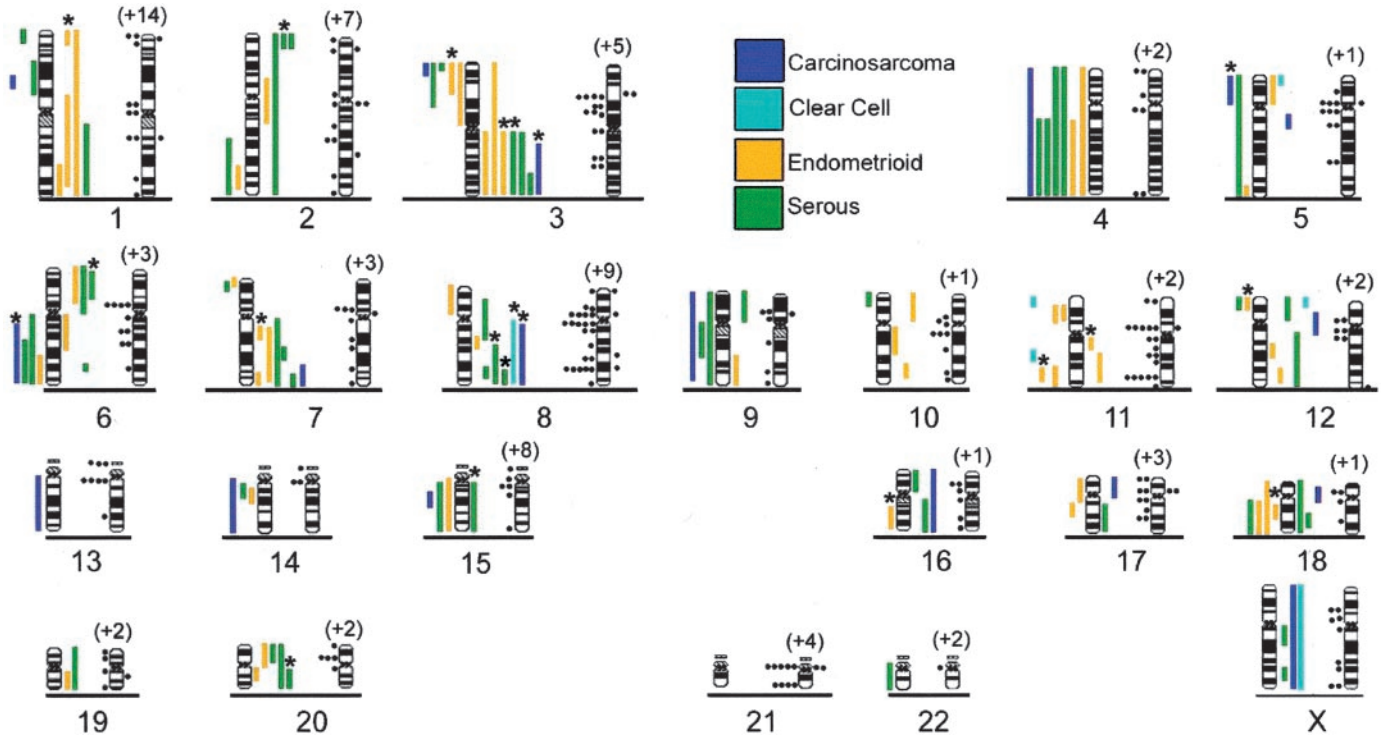

Fig. 2. Distribution of SKY and CGH aberrations based on the analysis of nine ovarian carcinoma patients. SKY results are summarized where *circles to the left of the ideogram* (*right ideogram* of each pair) indicate a site of clonal rearrangement. *Circles to the right of the ideogram* indicate a probable site of rearrangement based on limited banding information, and *numbers in parentheses above the ideogram* indicate the additional number of times that chromosome was involved in a clonal chromosomal rearrangement but where a breakpoint locus could not be readily identified. CGH results are summarized with *color-coded bars* denoting the histopathological subtype as described in the legend. *Bars to the right of the ideogram* (*left ideogram* of each pair) indicates a net gain of chromosomal material, whereas *bars to the left of the ideogram* indicates a net loss of chromosomal material. Because the paired samples (OCA13, OCA15, and OCA21) showed similar CGH results, these results were counted only once. "*" denotes the CGH changes that are concordant with the location of unbalanced structural chromosomal rearrangements identified by SKY analysis.

(19)t(8;19) (?p11;q13),+der(19)(9pter→p13::19p13→q13::8?p11→p?). On the basis of the CGH findings, it is likely that the deleted region of 8p arises as a result of a complex translocation involving 19 and 13 (inverted DAPI banding suggests that this segment derives from 8p). The remainder of chromosome 8 was involved in at least 4 breakpoints on 8 from the 8q21 region because this was detected as a regional gain by CGH. Imbalances identified by CGH analysis (Fig. 2) detected frequent chromosomal gains at 3q (58.3%), 8q (50%), 7q (50%), 20 (41.6%), 1q (33.3%), and 6p (25%). The most frequent losses were detected in chromosomes 4 (58.3%), 3p (41.6%), 6q (33.3%), and 18q (33.3%). The minimal common regions of chromosomal gains were identified at 1q21-q44, 3q13.3-q29, 6p21.2-p23, 7q32-q36, 8q23-q24.3, and 20p, whereas the minimal region of common loss was identified as 3p14-p26, 4q, 6q21-q27, and 18q12-q22.

To determine an integrated overall chromosomal distribution of genomic rearrangements as identified by both SKY and CGH, the total number of aberrations per chromosome shown in Fig. 2 was enumerated, and 396 rearrangements were identified in the study group. When the distribution was normalized with respect to relative genomic length, chromosomes 3, 8, 11, 17, and 21 had the highest frequencies of structural and numerical aberrations identified by SKY and CGH. Analysis of these combined CGH and SKY data demonstrates that regions of chromosomal imbalance (as detected by CGH) were concordant with the locations of chromosomal breakpoints (as identified by SKY), particularly for chromosomes 3 and 8. Consistent losses distal to 3p21 and gains of 3q (detailed in Fig. 1*D*) in tumors OCA2, OCA3A, OCA15A/B, and OCA19 were observed, whereas tumors OCA3, OCA5, OCA19, and OCA21A/B all had both SKY and CGH aberrations of the 8q23-q24 regions (Fig. 1*E*).

Microarray Expression Analysis of Study Group. To determine whether patterns of gene expression could be associated with the chromosomal features associated with the study group and to explore expression profiling of the tumor samples, two series of microarray experiments were carried out. At the time we began this study, normal ovary RNA was not available to us (commercially or otherwise). Therefore, in a first series of experiments, 13 ovarian tumors were analyzed by microarray using a pool of RNA derived from nine cell lines as an internal standard. When used in conjunction with two-dimensional average linkage unsupervised clustering, this approach allows the determination of relative gene expression profiles in multiple samples and is commonly used in microarray studies (40, 43–45). The results of the two-dimensional hierarchical clustering for this first series of experiments is presented in Fig. 3*A*. Profiles from primary tumor and metastasis isolated from the same patient, irrespective of biopsy time and anatomical site, showed the greatest similarity and always clustered close together as shown previously (27, 40, 46–50), indicating the robustness of the clustering algorithm. Consistent grouping of poorly differentiated tumors within this tumor set was seen independent of histological subtypes. Surprisingly, OCA15A/B, also a poorly differentiated tumor, clustered with the

to breakpoints as determined by SKY analysis. For each specimen, the classified SKY image is displayed for each chromosomal aberration that contributes to the net gain or loss of material from chromosome 3. *E*, integrated CGH and SKY analysis for chromosome 8. Shown are the tumor specimens possessing net genomic changes on chromosome 8 (denoted by "*") and are concordant with breakpoints as determined by SKY analysis. For each specimen, the classified SKY image is displayed for each chromosomal aberration that contributes to the net gain or loss of material from chromosome 8.

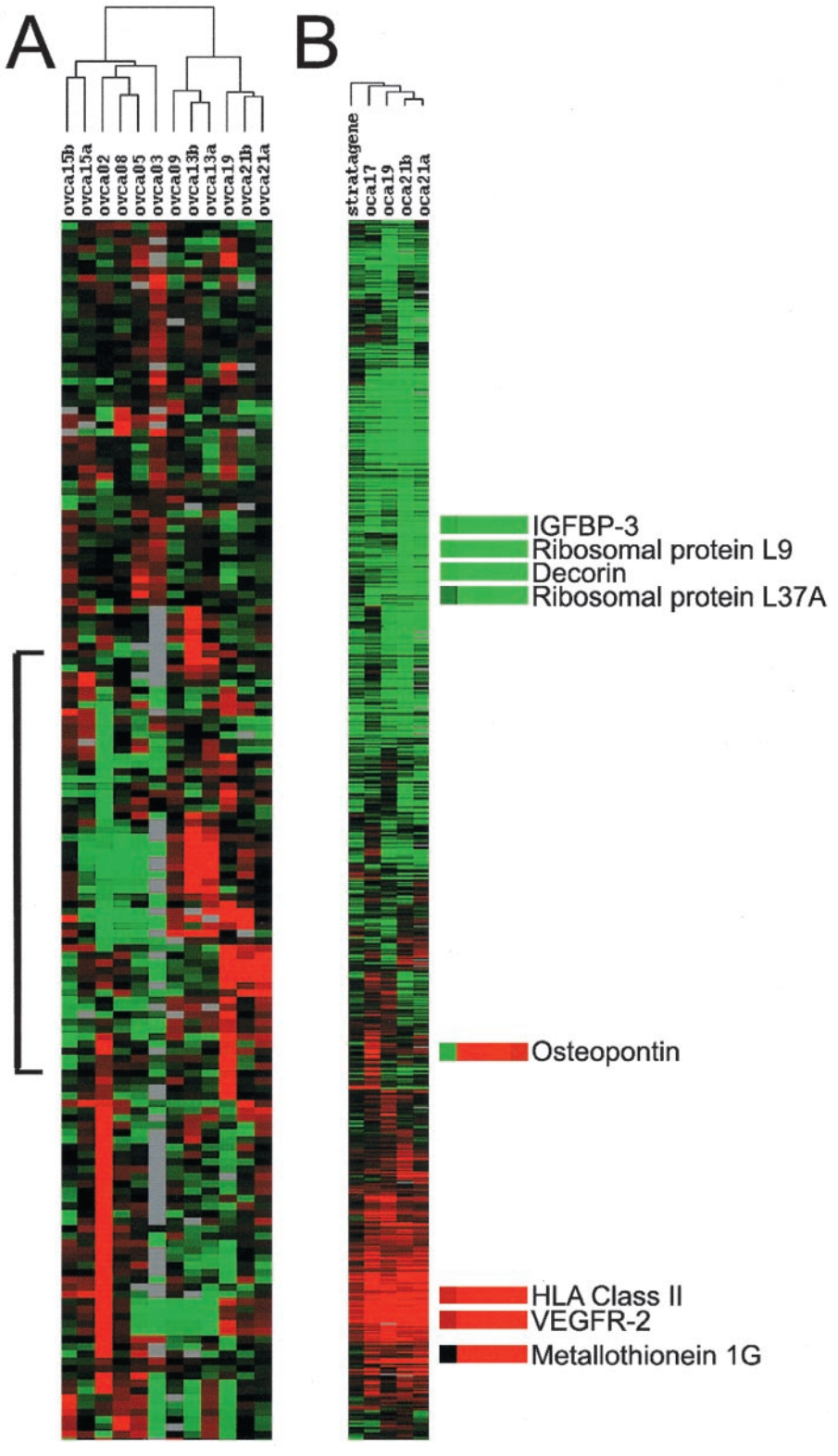

Fig. 3. Clustered display of data from ovarian cancer expression analysis. Data were measured using a cDNA microarray with elements representing ~1718 distinct human cDNAs. A larger version of these images with full gene names are available.[12] *A*, expression analysis of 13 ovarian tumors compared with the NCI9 tumor panel. The most informative part of the *dendrogram* is shown and produced as described in the text. Each gene is represented by a single row of *colored boxes*; each tumor is represented by a *single column*. In the color scale, *red squares* represent log expression ratios > 0 (overexpressed in the tumor), whereas *green squares* represent log expression ratios < 0 (underexpressed in the tumor). The color scale of saturation is proportional to the magnitude of the log expression ratio from the median value, with *red* indicating the greatest overexpression and *green* indicating the greatest underexpression. *Black squares* represent log expression ratios of 0 (similar expression in both tumor and reference), whereas *gray squares* indicate insufficient data. The algorithm used successively joins gene expression profiles to form a dendrogram based on their pairwise similarities. The poorly differentiated ovarian tumors in general cluster to the *right* (*vertical black bar* identifies an example block of gene expression that contributes to this cluster grouping). *B*, expression analysis of a subset of tumor samples and one normal ovary sample using normal ovary RNA as a common reference. Two separate clusters (I and II) are indicated by the similarity of the coloring of the corresponding regions of the *dendrogram*. Some differentially expressed genes in each cluster are shown on the *right side* of the colored image.

well-differentiated tumors. In addition, the three tumor pairs of karyotypically related tumors (OCA13A/B, OCA15A/B, and OCA21A/B) exhibited similar profiles and each tumor pair clustered together.

In a second series of microarray experiments, we studied the expression profiles of a subset of 4 ovarian tumor samples OCA17, OCA19, OCA21A, and OCA21B, as well as 1 normal ovary RNA sample (Stratagene RNA). We added to this subset of tumor samples a normal ovary RNA sample to assess variability between normal ovary RNA samples from different individuals. For these 5 samples, we used normal ovary RNA from a second commercial source (Ambion RNA) as a common reference, which allowed us to explore gene expression differences at the gene level between normal ovarian tissue and ovarian tumor tissue and to attempt a better correlation with the SKY and CGH results. Two-dimensional hierarchical clustering of the

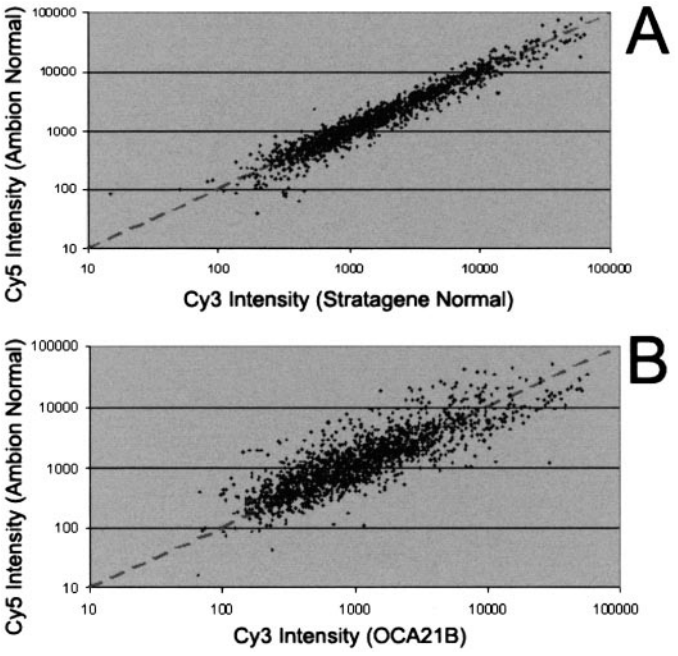

Fig. 4. Scatter plot of normalized intensities (log scale) for Stratagene normal ovary sample *versus* Ambion normal ovary sample (*A*) and tumor sample OCA21B *versus* Ambion normal ovary sample (*B*). A significantly broader scatter plot was observed in *B* than in *A*, indicating that the intrinsic variability between ovarian samples ("background noise") is small as compared with the difference in expression profiles observed when comparing tumor ovarian samples to normal ovarian samples.

microarray data showed that, as observed in the first series of microarray experiments, profiles from primary tumor and metastasis (OCA21A and OCA21B) obtained from the same patient showed the greatest similarity. Sample OCA19 showed an expression profile closely related to the one of OCA21A/B, similarly to what was observed when a pool of cell lines was used as a reference. Taken together, these results provide additional validation of the approach of using a pool of cell lines as an internal standard when studying global gene expression differences within a set of biological samples. Sample OCA17, which was not included in the first series of microarray experiments, shows a profile of expression slightly different from the 3 other tumor samples. As expected, the Stratagene normal ovary sample showed a gene expression profile very distinct from the 4 tumor samples and showed the least changes of gene expression as compared with the Ambion normal ovary RNA used as a reference. This result is illustrated in Fig. 4.

Two main clusters of gene expression were observed, designated I and II (Fig. 3*B*). A total of 194 genes showed expression levels that changed by more than a factor of two across the 4 tumor samples with 93 genes showing up-regulation and 101 genes showing down-regulation. We are currently exploring a number of these differentially expressed genes and chose to focus on a subset in the present publication.

Among the genes that showed up-regulation in the tumor samples (cluster I) was the gene encoding the OPN precursor, which showed a 53-fold increase in expression in sample OCA17 and a 2-fold increase in the other tumor samples. Five genes encoding metallothionein showed up-regulation (average ratios between tumor samples between 7.01 for MT-II and 2.87 for MT-1H), as well as gene encoding for the VEGF receptor 2 precursor (average ratio, 3.17), caspase-8 precursor (average ratio, 3.13), MYB-related protein (average ratio, 2.57), and six HLA class II histocompatibility antigens (average ratios between 3.66 and 2.23). Among the genes that showed down-regulation in the tumor samples (cluster II), there were 19 transcripts encoding 60S and 40S ribosomal proteins (average ratios between 0.49 and 0.23), IGFBP-3 (average ratio, 0.34), IGFBP-4 precursor (average ratio of 0.28), tumor necrosis factor α-induced protein 1 (average ratio, 0.26), G2/mitotic specific cyclin 2 (average ratio, 0.25), and decorin (average ratio, 0.15). The expression level of a subset of the differentially expressed genes was analyzed by semiquantitative RT-PCR. For OPN, decorin, and the ribosomal 60S L19 gene, the levels of overexpression or underexpression relative to a normal ovary were consistent with the levels determined by microarray expression analysis.[2]

Microarray Expression Analysis of cDNAs Mapping to Chromosomes 3 and 8. Because both the literature and our parallel SKY and CGH analysis have identified elevated frequencies of rearrangement and imbalance on chromosomes 3 and 8, we performed a detailed analysis of the results of ovarian cancer expression levels relative to a normal ovary for serous-derived tumors OCA17, OCA19, and OCA21A. A total of 94 and 51 targets represented genes with specific Blast and UniGene chromosomal band assignments on chromosomes 3 and 8, respectively, on the 1.7K3 cDNA array (Table 3). There was a contiguous distribution of reduced expression of seven genes mapping to 3p25.5–3p21.3 interval and increased expression of four genes from 3q13.33–3q28. These expression data were consistent with the observed pattern of CGH loss in distal 3p and gain in 3q observed both in this study and in the literature. Similarly, CGH data have consistently showed frequent gain and amplification in the 8q23–24 region in ovarian cancer, and the Exostosin Type I gene mapping to 8q23 exhibited increased expression in all three tumors.

DISCUSSION

This is the first cytogenetic study of short-term cultured ovarian chromosomal preparations using SKY and CGH methods (Table A).[15] The combined findings of this study (Fig. 2; Table 2) identified chromosomes 3, 8, 11, 17, and 21 as having the highest frequencies of structural and numerical aberrations identified by SKY and CGH. More evident were concordant CGH and SKY aberrations leading to losses distal to 3p21 and gains of 3q and of the region 8q23-q24 arising as a consequence of unbalanced structural rearrangements. In addition, other regions of rearrangement on chromosomes 1, 7, 12, 13, and 19 previously identified by G-banded chromosomal analysis (12, 13) were also noted. One-third more structural chromosomal aberrations were identified in the endometrioid tumors than the serous tumors. The poorly differentiated tumors, irrespective of histological subtype, showed twice as many chromosomal aberrations as the more well-differentiated tumors.

Previous conventional cytogenetic analysis has identified frequent breakage at 1p1, 1q1, 1p2, 1q2, 1p3, 1q3, 3p1, 1q4, 6q1, 6p2, 6q2, 7p1, 7p2, 11p1, 11q2, 12p1, 12q2, 13p1, and 19q (12). Similarly, loss of heterozygosity studies by Launonen *et al.* (51) have identified an association between loss of sequences at 3p14.2, 11p15.5, 11q23.2-q24, 16q24.3, and 17p13.1 and adverse outcome. The resulting loss of heterozygosity in these and other regions can result from simple deletions or deletions as a result of translocations. Because SKY can identify cryptic translocations and poorly resolved "marker chromosomes" with greater certainty, a much more accurate picture of overall cytogenetic change is possible. Many chromosomal translocations were centromeric or pericentromeric, suggesting the involvement of repetitive centromeric sequences or *Alu* repeats that may facilitate rearrangements leading to chromosomal imbalance (52). Chromosomal breakage at 1p1* and 3q* occur in ovarian cancer (5, 7, 11) and confers a poor outcome (13).

[15] Table A to be available as supplementary on the web edition. Full description of SKY and CGH results.

Table 3 *Distribution of overexpressed and underexpressed genes mapping to chromosomes 3 and 8*

Shown are the gene name, symbol, chromosomal location, and expression level results of the gene from the 1.7K3 microarray expression analysis of serous type tumors OCA17, OCA19 and OCA21A for chromosomes 3 and 8. Only genes showing concordant up-regulation or down-regulation in comparison with a normal ovary for all three tumors are shown. Genes mapping to chromosomal locations that are consistently lost (3p) or gained (3q and distal 8q) are shown in bold.

Name	Symbol	Accession no.	−Megabase (from pter)	Locus	OCA17	OCA19	OCA21A
					Expression (fold change)		
Ribosomal protein L32	**RPL32**	**W24343**	**15.66**	**3p25.1**	**−2.70**	**−1.94**	**−2.57**
Hypothetical protein	**KIAA0084**	**AA127738**	**19.49**	**3p24.3**	**−2.02**	**−2.19**	**−2.14**
Transforming growth factor beta Receptor Type II	**TGFBR2**	**AA028183**	**31.31**	**3p22.3**	**−1.35**	**−1.92**	**−2.38**
ADP/ATP translocase 3	**ANT3**	**AA017412**	**~39.14**	**3p21.32**	**−1.59**	**−2.22**	**−3.85**
Vasoactive intestinal polypeptide receptor 1	**VIPR1**	**H14880**	**43.27**	**3p21.32**	**−1.59**	**−1.87**	**−2.06**
Microtubule-associated protein 4	**MAP4**	**H50895**	**48.68**	**3p21.31**	**−1.59**	**−1.59**	**−2.86**
Laminin, β2	**LAMS**	**AA029359**	**~50.25**	**3p21.31**	**−3.04**	**−2.23**	**−2.97**
Glycogen branching enzyme	GBE1	T98705	84.98	3p12.2	+2.67	+2.39	+2.74
Ribosomal protein L24	RPL24	N94916	103.73	3q12.3	−1.96	−1.97	−2.62
Homogentisate 1,2-dioxygenase	**HGD**	**T83013**	**123.39**	**3q13.33**	**+2.32**	**+2.83**	**+2.64**
Calcium-sensing receptor	**CASR**	**W56898**	**125.28**	**3q21.1**	**+2.43**	**+2.96**	**+2.58**
Transmembrane 4 superfamily member 4	**TM4SF**	**T83911**	**154.04**	**3q25.1**	**+4.35**	**+1.32**	**+1.47**
Somatostatin	**SST**	**R20699**	**193.05**	**3q28**	**+1.04**	**+4.83**	**+1.00**
Farnesyldiphosphate farnesyltransferase 1	FDFT1	W94208	11.24	8p23.1	−1.56	−2.07	−2.21
Dual specificity mitogen-activated protein kinase kinase 1	MAPKK1	T87961	30.51	8p12	+2.42	+3.04	+3.08
Serine/threonine protein phosphatase	P2AB	N31088	~31.75	8p12	−1.67	−2.08	−1.57
Tissue plasminogen activator	TPA	H10533	42.80	8p11.1	−1.55	−1.84	−2.00
Minichromosome maintenance, homologue of CDC21	MCM4	N35453	46.71	8q11.21	+3.41	+2.70	+2.39
CCAAT/enhancer-binding protein, δ	CEBPD	AA044627	46.90	8q11.21	−1.25	−2.25	−3.33
Hypothetical protein	KIAA0112	AA147503	65.76	8q12.3	+2.34	+1.00	+1.45
MYB-related protein A	MYBA	H13357	65.87	8q12.3	+2.00	+3.35	+2.48
Myo-inositol monophosphatase 1	IMPA1	H03789	81.02	8q21.13	+1.30	+2.11	+1.03
Serine exchange enzyme	PSS1	T80295	95.97	8q22.1	+2.44	+2.68	+2.10
Syndecan-2	SDC2	AA114890	96.25	8q22.1	−3.49	−2.07	−2.72
Exostosin Type I	**EXT**	**W03422**	**117.25**	**8q23**	**+2.66**	**+3.28**	**+2.85**
Zinc finger protein 7	ZNF7	AA005274	142.96	8q24.3	−1.11	−2.51	−1.93

Ovarian cancer often presents in more than one site or has metastasized at the time of surgery. We studied the chromosomal and gene expression patterns in tumors arising in two sites to determine their common origin. In three instances, two separate tumors were available for simultaneous analysis of patterns of gene expression and karyotypes. In all three pairs, there was a marked similarity in the chromosomal constitution of the tumors and each tumor pair clustered together on the dendrogram obtained with microarray analysis. One tumor pair presented an interesting opportunity to determine cytogenetic changes during metastasis. OCA21 possessed a tetraploid primary tumor and a diploid karyotype in the metastatic tumor, suggesting that either a reduction in chromosomal ploidy occurred in the primary tumor before metastasis or that the reduction occurred at the metastatic site. The cytogenetic description of the metastatic biopsy is similar to components of structural alterations observed in the primary tumor, suggesting that a selection of a dominant clone with specific structural abnormalities arose in the metastatic tumor.

The minimal regions of chromosomal imbalance identified by CGH were gains at 1q21-q44, 3q13.3-q29, 6p21.2-p23, 7q32-q36, and 8q23-q24.3 and losses at 3p14-p26, 4q, 6q21-q27, and 18q12-q22. Previous CGH studies (17–24) have identified a similar pattern of genomic change, and attempts have been made to correlate these data with clinical endpoints (53). Studies by Yonescu *et al.* (54) and Jenkins *et al.* (11) show that structural and numerical changes predominantly occur on chromosome 11 endometrioid tumors. The high percentage of chromosome 4 loss (58.3%) is consistent with literature reports of chromosome 4 involvement in advanced staged tumors (18).

The expression clustering of genes/pathways may elucidate those critical genes that promote both a more aggressive disease course and worse outcome and may provide a marker for treatment resistance. The first series of microarray experiments described here consisted of analyzing 13 tumor samples using a pool of nine cell lines as a common reference. Two-dimensional hierarchical clustering identified a grouping of predominantly poorly differentiated subtypes (OCA13A/B, OCA19, and OCA21A/B), which were independent of histological grouping. The only discrepancy was the tumor OCA15 that failed to cluster with the other poorly differentiated tumors in the study group. It is possible that histological heterogeneity or the lower quantity of RNA obtained for this particular tumor sample resulted in this grouping obtained by cluster analysis.

The second series of microarray experiments carried out on a subset of tumor samples and using normal ovarian tissue as a common reference identified 194 genes differentially expressed at a level of at least 2 (up or down) between tumor samples and the reference normal sample. Two-dimensional hierarchical clustering and statistical analysis revealed a very similar expression profile for all 4 tumor samples, with only 13% of genes showing a SD $>$ 1 across all tumor samples, consistent with their similar serous histology (OCA17, OCA19, and OCA21A/B). As expected, the normal ovary sample used as a negative control displayed very few significantly differentially expressed genes when compared with the normal reference (Fig. 4).

One of the objectives of this study was to identify correlations between gene expression deviations observed by microarray analysis and chromosomal imbalances identified by CGH. Because chromosomes 3 and 8 have been previously shown to be subject to rearrangement and copy number change (12–14) and were found to be commonly involved in rearrangements by SKY and/or CGH, we performed a more detailed expression evaluation of cDNA mapping to these chromosomes. We identified a contiguous distribution of reduced expression of seven genes mapping to 3p25.5–3p21.3 interval and increased expression of four genes from 3q13.33–3q28 that were consistent with loss of 3p and gain of 3q in this and other CGH studies of ovarian cancer (17–25). Within the 3q13.33–3q28 interval, it is noteworthy that there was elevated expression of the calcium-sensing receptor (55) that has been previously shown to induce human ovarian surface epithelial cells to modulate extracellular calcium and induce proliferation.

Two-dimensional hierarchical clustering revealed two large clusters of expression profiles (I and II, Fig. 3*B*). The first cluster consists of up-regulated genes and most striking is the very high value (ratio of 53) obtained for the OPN precursor in sample OCA17. This gene is also overexpressed in the other tumor samples but to a much lesser

extent. OPN is a noncollagenous bone-related protein that has been detected by immunohistochemical and *in situ* hybridization in calcified psammona bodies, which frequently occur in ovarian serous papillary tumors (56). This protein may be causally related with the calcification of the psammona bodies of the ovarian serous papillary tumors such as OCA17. Five genes encoding metallothionein are also up-regulated in all 4 tumor samples. Metallothionein is a key component of platinum resistance in epithelial ovarian cancer and is thought to be of prognostic significance (57).

Cluster I also contains five genes encoding HLA class II histocompatibility antigens. All five genes are located in the 6p region, which was involved in genomic imbalance and structural rearrangement, so it was of interest that MHC class II genes of the leukocyte antigen (HLA) complex emerges as a strong cluster of expression. This observation is in agreement with a recent high-density filter array analysis of ovarian cancer, which also reported differential expression of immune response mediators (58). Previously, an association between the T-cell response and alterations to MHC expression has been observed in ovarian cancer (59, 60). However, it is conceivable that infiltrating lymphocyte may also contribute to overexpression of immune response genes.

The VEGF receptor 2 precursor is up-regulated in all tumor samples, and this is consistent with a previous cDNA microarray study (58) on four poorly differentiated serous papillary tumors that showed an overall increase in angiogenesis-related markers, including VEGF.

Among the down-regulated genes, we identified 19 genes encoding ribosomal proteins. Ribosomal proteins have been found to be up-regulated in some tumor tissues (61). However, a recent study (62) using a data mining tool called Digital Differential Display has shown that distinct ribosomal proteins were found to be up-regulated and down-regulated in a tumor type-dependent manner. In that study, some ribosomal proteins (S15A, S17, and L35) were found to be up-regulated in breast and prostate carcinoma-derived libraries, whereas others such as L9, L23, and L37A were down-regulated in ovarian cancer-derived libraries. Our present findings are consistent with these results. IGFBP-3 precursor showed down-regulation in all tumor samples as observed by others (63). Finally, the gene encoding a decorin precursor showed the highest level of down-regulation. Decorin is a small proteoglycan protein, which is part of the cellular matrix and has been shown to inhibit the growth of two ovarian cell lines *in vitro* (64). Decorin inhibits transforming growth factor β and induces p21, resulting in inhibition of proliferation (65). A marked decrease in the endogenous level of decorin precursor might therefore result in an increase in cell proliferation in tumor cells.

A more complete cytogenetic and microarray analysis of a larger collection of ovarian tumor and normal samples and using cDNA microarrays spotted with 19,200 genes and ESTs is under way in our laboratories that will allow us to uncover additional differentially expressed genes and to further explore the ones identified in the present study,[16] as well as additional regions of chromosomal instability associated with ovarian cancer. In this study, we performed a comparative analysis using SKY, CGH, and microarrays on a small cohort of ovarian carcinomas. We showed that chromosomes 3, 8, 11, 17, and 21 had the highest overall frequencies of structural and numerical aberrations and losses distal to 3p21, and consistent gains of 3q were associated with a pattern of reduced expression of genes mapping to 3p25.5–3p21.3 and increased expression of genes from 3q13.33–3q28. Thus, although there is inherently limited resolution of all cytogenetically based techniques, we have shown that a parallel strategy of genomic and expression analysis can facilitate the identification of smaller subsets of genes pertinent to ovarian cancer.

ACKNOWLEDGMENTS

We thank Drs. Kathy Chun, Ajay Pandita, Dan Grisaru, and Jim Woodgett for critically reading this manuscript.

REFERENCES

1. Holschneider, C. H., and Berek, J. S. Ovarian cancer: epidemiology, biology, and prognostic factors. Semin. Surg. Oncol., *19:* 3–10, 2000.
2. Morita, K., Ono, Y., Fukui, H., Tomita, S., Ueda, Y., Terano, A., and Fujimori, T. Incidence of P53 and K-*ras* alterations in ovarian mucinous and serous tumors. Pathol. Int., *50:* 219–223, 2000.
3. Obata, K., Morland, S. J., Watson, R. H., Hitchcock, A., Chenevix-Trench, G., Thomas, E. J., and Campbell, I. G. Frequent PTEN/MMAC mutations in endometrioid but not serous or mucinous epithelial ovarian tumors. Cancer Res., *58:* 2095–2097, 1998.
4. Pejovic, T., Himmelmann, A., Heim, S., Mandahl, N., Floderus, U. M., Furgyik, S., Elmfors, B., Helm, G., Willen, H., and Mitelman, F. Prognostic impact of chromosome aberrations in ovarian cancer. Br. J. Cancer, *65:* 282–286, 1992.
5. Pejovic, T., Heim, S., Mandahl, N., Baldetorp, B., Elmfors, B., Floderus, U. M., Furgyik, S., Helm, G., Himmelmann, A., Willen, H., *et al*. Chromosome aberrations in 35 primary ovarian carcinomas. Genes Chromosomes Cancer, *4:* 58–68, 1992.
6. Thompson, F. H., Liu, Y., Emerson, J., Weinstein, R., Makar, R., Trent, J. M., Taetle, R., and Alberts, D. S. Simple numeric abnormalities as primary karyotype changes in ovarian carcinoma. Genes Chromosomes Cancer, *10:* 262–266, 1994.
7. Thompson, F. H., Emerson, J., Alberts, D., Liu, Y., Guan, X. Y., Burgess, A., Fox, S., Taetle, R., Weinstein, R., Makar, R., *et al*. Clonal chromosome abnormalities in 54 cases of ovarian carcinoma. Cancer Genet. Cytogenet., *73:* 33–45, 1994.
8. Thompson, F. H., Nelson, M. A., Trent, J. M., Guan, X. Y., Liu, Y., Yang, J. M., Emerson, J., Adair, L., Wymer, J., Balfour, C., Massey, K., Weinstein, R., Alberts, D. S., and Taetle, R. Amplification of 19q13.1-q13.2 sequences in ovarian cancer. G-band, FISH, and molecular studies. Cancer Genet. Cytogenet., *87:* 55–62, 1996.
9. Thompson, F. H., Taetle, R., Trent, J. M., Liu, Y., Massey-Brown, K., Scott, K. M., Weinstein, R. S., Emerson, J. C., Alberts, D. S., and Nelson, M. A. Band 1p36 abnormalities and t(1;17) in ovarian carcinoma. Cancer Genet. Cytogenet., *96:* 106–110, 1997.
10. Whang-Peng, J., Knutsen, T., Douglass, E. C., Chu, E., Ozols, R. F., Hogan, W. M., and Young, R. C. Cytogenetic studies in ovarian cancer. Cancer Genet. Cytogenet., *11:* 91–106, 1984.
11. Jenkins, R. B., Bartelt, D., Jr., Stalboerger, P., Persons, D., Dahl, R. J., Podratz, K., Keeney, G., and Hartmann, L. Cytogenetic studies of epithelial ovarian carcinoma. Cancer Genet. Cytogenet., *71:* 76–86, 1993.
12. Taetle, R., Aickin, M., Yang, J. M., Panda, L., Emerson, J., Roe, D., Adair, L., Thompson, F., Liu, Y., Wisner, L., Davis, J. R., Trent, J., and Alberts, D. S. Chromosome abnormalities in ovarian adenocarcinoma: I. Nonrandom chromosome abnormalities from 244 cases. Genes Chromosomes Cancer, *25:* 290–300, 1999.
13. Taetle, R., Aickin, M., Panda, L., Emerson, J., Roe, D., Thompson, F., Davis, J., Trent, J., and Alberts, D. Chromosome abnormalities in ovarian adenocarcinoma: II. Prognostic impact of nonrandom chromosome abnormalities in 244 cases. Genes Chromosomes Cancer, *25:* 46–52, 1999.
14. Simon, R., Desper, R., Papadimitriou, C. H., Peng, A., Alberts, D. S., Taetle, R., Trent, J. M., and Schaffer, A. A. Chromosome abnormalities in ovarian adenocarcinoma: III. Using breakpoint data to infer and test mathematical models for oncogenesis. Genes Chromosomes Cancer, *28:* 106–120, 2000.
15. Lichter, P., Joos, S., Bentz, M., and Lampel, S. Comparative genomic hybridization: uses and limitations. Semin. Hematol., *37:* 348–357, 2000.
16. Bayani, J., and Squire, J. Advances in the detection of chromosomal aberrations using spectral karyotyping. Clin. Genet., *59:* 65–73, 2001.
17. Wasenius, V. M., Jekunen, A., Monni, O., Joensuu, H., Aebi, S., Howell, S. B., and Knuutila, S. Comparative genomic hybridization analysis of chromosomal changes occurring during development of acquired resistance to cisplatin in human ovarian carcinoma cells. Genes Chromosomes Cancer, *18:* 286–291, 1997.
18. Sonoda, G., Palazzo, J., du Manoir, S., Godwin, A. K., Feder, M., Yakushiji, M., and Testa, J. R. Comparative genomic hybridization detects frequent overrepresentation of chromosomal material from 3q26, 8q24, and 20q13 in human ovarian carcinomas. Genes Chromosomes Cancer, *20:* 320–328, 1997.
19. Tapper, J., Sarantaus, L., Vahteristo, P., Nevanlinna, H., Hemmer, S., Seppala, M., Knuutila, S., and Butzow, R. Genetic changes in inherited and sporadic ovarian carcinomas by comparative genomic hybridization: extensive similarity except for a difference at chromosome 2q24–q32. Cancer Res., *58:* 2715–2719, 1998.
20. Riopel, M. A., Spellerberg, A., Griffin, C. A., and Perlman, E. J. Genetic analysis of ovarian germ cell tumors by comparative genomic hybridization. Cancer Res., *58:* 3105–3110, 1998.
21. Wolf, N. G., Abdul-Karim, F. W., Farver, C., Schrock, E., du Manoir, S., and Schwartz, S. Analysis of ovarian borderline tumors using comparative genomic hybridization and fluorescence *in situ* hybridization. Genes Chromosomes Cancer, *25:* 307–315, 1999.
22. Suehiro, Y., Sakamoto, M., Umayahara, K., Iwabuchi, H., Sakamoto, H., Tanaka, N., Takeshima, N., Yamauchi, K., Hasumi, K., Akiya, T., Sakunaga, H., Muroya, T.,

[16] D. Grisaru, M. Albert, J. Goncalves, J. Woodgett, J. A. Squire, K. J. Murphy, B. Rosen, A. Covens, R. Osborne, H. Begley, P. Shaw, and P. F. Macgregor. Prognostic prediction in advanced serous epithelial ovarian cancer using molecular profiling, manuscript in preparation.

Numa, F., Kato, H., Tenjin, Y., and Sugishita, T. Genetic aberrations detected by comparative genomic hybridization in ovarian clear cell adenocarcinomas. Oncology (Basel), *59:* 50–56, 2000.
23. Patael-Karasik, Y., Daniely, M., Gotlieb, W. H., Ben-Baruch, G., Schiby, J., Barakai, G., Goldman, B., Aviram, A., and Friedman, E. Comparative genomic hybridization in inherited and sporadic ovarian tumors in Israel. Cancer Genet. Cytogenet., *121:* 26–32, 2000.
24. Shayesteh, L., Lu, Y., Kuo, W. L., Baldocchi, R., Godfrey, T., Collins, C., Pinkel, D., Powell, B., Mills, G. B., and Gray, J. W. PIK3CA is implicated as an oncogene in ovarian cancer [see comments]. Nat. Genet., *21:* 99–102, 1999.
25. Shridhar, V., Lee, J., Pandita, A., Iturria, S., Avula, R., Staub, J., Morrissey, M., Calhoun, E., Sen, A., Kalli, K., Keeney, G., Roche, P., Cliby, W., Lu, K., Schmandt, R., Mills, G. B., Bast, R. C., Jr., James, C. D., Couch, F. J., Hartmann, L. C., Lillie, J., and Smith, D. I. Genetic analysis of early- *versus* late-stage ovarian tumors. Cancer Res., *61:* 5895–5904, 2001.
26. Shalon, D., Smith, S. J., and Brown, P. O. A DNA microarray system for analyzing complex DNA samples using two-color fluorescent probe hybridization. Genome Res., *6:* 639–645, 1996.
27. DeRisi, J., Penland, L., Brown, P. O., Bittner, M. L., Meltzer, P. S., Ray, M., Chen, Y., Su, Y. A., and Trent, J. M. Use of a cDNA microarray to analyse gene expression patterns in human cancer [see comments]. Nat. Genet., *14:* 457–460, 1996.
28. Ono, K., Tanaka, T., Tsunoda, T., Kitahara, O., Kihara, C., Okamoto, A., Ochiai, K., Takagi, T., and Nakamura, Y. Identification by cDNA microarray of genes involved in ovarian carcinogenesis. Cancer Res., *60:* 5007–5011, 2000.
29. Wang, K., Gan, L., Jeffery, E., Gayle, M., Gown, A. M., Skelly, M., Nelson, P. S., Ng, W. V., Schummer, M., Hood, L., and Mulligan, J. Monitoring gene expression profile changes in ovarian carcinomas using cDNA microarray. Gene (Amst.), *229:* 101–108, 1999.
30. Welsh, J. B., Zarrinkar, P. P., Sapinoso, L. M., Kern, S. G., Behling, C. A., Monk, B. J., Lockhart, D. J., Burger, R. A., and Hampton, G. M. Analysis of gene expression profiles in normal and neoplastic ovarian tissue samples identifies candidate molecular markers of epithelial ovarian cancer. Proc. Natl. Acad. Sci. USA, *98:* 1176–1181, 2001.
31. Hough, C. D., Sherman-Baust, C. A., Pizer, E. S., Montz, F. J., Im, D. D., Rosenshein, N. B., Cho, K. R., Riggins, G. J., and Morin, P. J. Large-scale serial analysis of gene expression reveals genes differentially expressed in ovarian cancer. Cancer Res., *60:* 6281–6287, 2000.
32. Hough, C. D., Cho, K. R., Zonderman, A. B., Schwartz, D. R., and Morin, P. J. Coordinately up-regulated genes in ovarian cancer. Cancer Res., *61:* 3869–3876, 2001.
33. Dracopoli, N. C. Current Protocols in Human Genetics. New York: John Wiley & Sons, Inc., 2001.
34. Chomczynski, P., and Sacchi, N. Single-step method of RNA isolation by acid guanidinium thiocyanate-phenol-chloroform extraction. Anal. Biochem., *162:* 156–159, 1987.
35. Ross, D. T., Scherf, U., Eisen, M. B., Perou, C. M., Rees, C., Spellman, P., Iyer, V., Jeffrey, S. S., Van de Rijn, M., Waltham, M., Pergamenschikov, A., Lee, J. C., Lashkari, D., Shalon, D., Myers, T. G., Weinstein, J. N., Botstein, D., and Brown, P. O. Systematic variation in gene expression patterns in human cancer cell lines. Nat. Genet., *24:* 227–235, 2000.
36. Schrock, E., du Manoir, S., Veldman, T., Schoell, B., Wienberg, J., Ferguson-Smith, M. A., Ning, Y., Ledbetter, D. H., Bar-Am, I., Soenksen, D., Garini, Y., and Ried, T. Multicolor spectral karyotyping of human chromosomes [see comments]. Science (Wash. DC), *273:* 494–497, 1996.
37. Mitelman, F. ISCN (1995): International System for Human Cytogenetic Nomenclature, p. 114. New York: S. Karger, 1995.
38. Kallioniemi, A., Kallioniemi, O. P., Sudar, D., Rutovitz, D., Gray, J. W., Waldman, F., and Pinkel, D. Comparative genomic hybridization for molecular cytogenetic analysis of solid tumors. Science (Wash. DC), *258:* 818–821, 1992.
39. Eisen, M. B., Spellman, P. T., Brown, P. O., and Botstein, D. Cluster analysis and display of genome-wide expression patterns. Proc. Natl. Acad. Sci. USA, *95:* 14863–14868, 1998.
40. Perou, C. M., Sorlie, T., Eisen, M. B., van de Rijn, M., Jeffrey, S. S., Rees, C. A., Pollack, J. R., Ross, D. T., Johnsen, H., Akslen, L. A., Fluge, O., Pergamenschikov, A., Williams, C., Zhu, S. X., Lonning, P. E., Borresen-Dale, A. L., Brown, P. O., and Botstein, D. Molecular portraits of human breast tumours. Nature (Lond.), *406:* 747–752, 2000.
41. Alon, U., Barkai, N., Notterman, D. A., Gish, K., Ybarra, S., Mack, D., and Levine, A. J. Broad patterns of gene expression revealed by clustering analysis of tumor and normal colon tissues probed by oligonucleotide arrays. Proc. Natl. Acad. Sci. USA, *96:* 6745–6750, 1999.
42. Heng, H. H., and Tsui, L. C. Modes of DAPI banding and simultaneous *in situ* hybridization. Chromosoma, *102:* 325–332, 1993.
43. Alizadeh, A. A., Eisen, M. B., Davis, R. E., Ma, C., Lossos, I. S., Rosenwald, A., Boldrick, J. C., Sabet, H., Tran, T., Yu, X., Powell, J. I., Yang, L., Marti, G. E., Moore, T., Hudson, J., Jr., Lu, L., Lewis, D. B., Tibshirani, R., Sherlock, G., Chan, W. C., Greiner, T. C., Weisenburger, D. D., Armitage, J. O., Warnke, R., Staudt, L. M., *et al*. Distinct types of diffuse large B-cell lymphoma identified by gene expression profiling. Nature (Lond.), *403:* 503–511, 2000.
44. Bittner, M., Meltzer, P., Chen, Y., Jiang, Y., Seftor, E., Hendrix, M., Radmacher, M., Simon, R., Yakhini, Z., Ben-Dor, A., Sampas, N., Dougherty, E., Wang, E., Marincola, F., Gooden, C., Lueders, J., Glatfelter, A., Pollock, P., Carpten, J., Gillanders, E., Leja, D., Dietrich, K., Beaudry, C., Berens, M., Alberts, D., and Sondak, V. Molecular classification of cutaneous malignant melanoma by gene expression profiling. Nature (Lond.), *406:* 536–540, 2000.
45. Alizadeh, A. A., and Staudt, L. M. Genomic-scale gene expression profiling of normal and malignant immune cells. Curr. Opin. Immunol., *12:* 219–225, 2000.
46. Kudoh, K., Ramanna, M., Ravatn, R., Elkahloun, A. G., Bittner, M. L., Meltzer, P. S., Trent, J. M., Dalton, W. S., and Chin, K. V. Monitoring the expression profiles of doxorubicin-induced and doxorubicin-resistant cancer cells by cDNA microarray. Cancer Res, *60:* 4161–4166, 2000.
47. Carlisle, A. J., Prabhu, V. V., Elkahloun, A., Hudson, J., Trent, J. M., Linehan, W. M., Williams, E. D., Emmert-Buck, M. R., Liotta, L. A., Munson, P. J., and Krizman, D. B. Development of a prostate cDNA microarray and statistical gene expression analysis package. Mol. Carcinog., *28:* 12–22, 2000.
48. Loftus, S. K., Chen, Y., Gooden, G., Ryan, J. F., Birznieks, G., Hilliard, M., Baxevanis, A. D., Bittner, M., Meltzer, P., Trent, J., and Pavan, W. Informatic selection of a neural crest-melanocyte cDNA set for microarray analysis. Proc. Natl. Acad. Sci. USA, *96:* 9277–9280, 1999.
49. Amundson, S. A., Bittner, M., Chen, Y., Trent, J., Meltzer, P., and Fornace, A. J., Jr. Fluorescent cDNA microarray hybridization reveals complexity and heterogeneity of cellular genotoxic stress responses. Oncogene, *18:* 3666–3672, 1999.
50. Khan, J., Bittner, M. L., Chen, Y., Meltzer, P. S., and Trent, J. M. DNA microarray technology: the anticipated impact on the study of human disease. Biochim. Biophys. Acta, *1423:* M17–M28, 1999.
51. Launonen, V., Mannermaa, A., Stenback, F., Kosma, V. M., Puistola, U., Huusko, P., Anttila, M., Bloigu, R., Saarikoski, S., Kauppila, A., and Winqvist, R. Loss of heterozygosity at chromosomes 3, 6, 8, 11, 16, and 17 in ovarian cancer: correlation to clinicopathological variables. Cancer Genet. Cytogenet., *122:* 49–54, 2000.
52. Beheshti, B., Karaskova, J., Park, P. C., Squire, J. A., and Beatty, B. G. Identification of a high frequency of chromosomal rearrangements in the centromeric regions of prostate cancer cell lines by sequential giemsa banding and spectral karyotyping. Mol. Diagn., *5:* 23–32, 2000.
53. Suzuki, S., Moore, D. H., II, Ginzinger, D. G., Godfrey, T. E., Barclay, J., Powell, B., Pinkel, D., Zaloudek, C., Lu, K., Mills, G., Berchuck, A., and Gray, J. W. An approach to analysis of large-scale correlations between genome changes and clinical endpoints in ovarian cancer. Cancer Res., *60:* 5382–5385, 2000.
54. Yonescu, R., Currie, J. L., Hedrick, L., Campbell, J., and Griffin, C. A. Chromosome abnormalities in primary endometrioid ovarian carcinoma. Cancer Genet. Cytogenet., *87:* 167–171, 1996.
55. McNeil, L., Hobson, S., Nipper, V., and Rodland, K. D. Functional calcium-sensing receptor expression in ovarian surface epithelial cells. Am. J. Obstet. Gynecol., *178:* 305–313, 1998.
56. Maki, M., Hirota, S., Kaneko, Y., and Morohoshi, T. Expression of osteopontin messenger RNA by macrophages in ovarian serous papillary cystadenocarcinoma: a possible association with calcification of psammoma bodies. Pathol. Int., *50:* 531–535, 2000.
57. Wrigley, E., Verspaget, H. W., Jayson, G. C., and McGown, A. T. Metallothionein expression in epithelial ovarian cancer: effect of chemotherapy and prognostic significance. J. Cancer Res. Clin. Oncol., *126:* 717–721, 2000.
58. Martoglio, A. M., Tom, B. D., Starkey, M., Corps, A. N., Charnock-Jones, D. S., and Smith, S. K. Changes in tumorigenesis- and angiogenesis-related gene transcript abundance profiles in ovarian cancer detected by tailored high density cDNA arrays. Mol. Med., *6:* 750–765, 2000.
59. Nagy, N., Vanky, F., and Klein, E. Tumor surveillance: expression of the transporter associated with antigen processing (TAP-1) in *ex vivo* human tumor samples and its elevation by *in vitro* treatment with IFN-γ and TNF-α. Immunol. Lett., *64:* 153–160, 1998.
60. Kono, K., Halapi, E., Hising, C., Petersson, M., Gerdin, E., Vanky, F., and Kiessling, R. Mechanisms of escape from CD8+ T-cell clones specific for the *HER-2/neu* proto-oncogene expressed in ovarian carcinomas: related and unrelated to decreased MHC class 1 expression. Int. J. Cancer, *70:* 112–119, 1997.
61. Vaarala, M. H., Porvari, K. S., Kyllonen, A. P., Mustonen, M. V., Lukkarinen, O., and Vihko, P. T. Several genes encoding ribosomal proteins are overexpressed in prostate cancer cell lines: confirmation of L7a and L37 overexpression in prostate cancer tissue samples. Int. J. Cancer, *78:* 27–32, 1998.
62. Scheurle, D., DeYoung, M. P., Binninger, D. M., Page, H., Jahanzeb, M., and Narayanan, R. Cancer gene discovery using digital differential display. Cancer Res., *60:* 4037–4043, 2000.
63. Katsaros, D., Yu, H., Levesque, M. A., Danese, S., Genta, F., Richiardi, G., Fracchioli, S., Khosravi, M. J., Diamandi, A., Gordini, G., Diamandis, E. P., and Massobrio, M. IGFBP-3 in epithelial ovarian carcinoma and its association with clinicopathological features and patient survival. Eur. J. Cancer, *37:* 478–485, 2001.
64. Nash, M. A., Loercher, A. E., and Freedman, R. S. *In vitro* growth inhibition of ovarian cancer cells by decorin: synergism of action between decorin and carboplatin. Cancer Res., *59:* 6192–6196, 1999.
65. Stander, M., Naumann, U., Wick, W., and Weller, M. Transforming growth factor β and p-21: multiple molecular targets of decorin-mediated suppression of neoplastic growth. Cell Tissue Res., *296:* 221–227, 1999.